Spectrochimica Acta Part A: Molecular and Biomolecular Spectroscopy 173 (2017) 182–187

Contents lists available at ScienceDirect

Spectrochimica Acta Part A: Molecular and Biomolecular Spectroscopy

journal homepage: www.elsevier.com/locate/saa

Electronic states of Myricetin. UV–Vis polarization spectroscopy and quantum chemical calculations☆

Danijela Vojta [a,*], Eva Marie Karlsen [b], Jens Spanget-Larsen [b,*]

[a] Division of Organic Chemistry and Biochemistry, Rudjer Boskovic Institute, Bijenicka 54, 10000 Zagreb, Croatia
[b] Department of Science and Environment, Roskilde University, Postbox 260, Universitetsvej 1, DK-4000 Roskilde, Denmark

ARTICLE INFO

Article history:
Received 14 July 2016
Received in revised form 10 September 2016
Accepted 12 September 2016
Available online 13 September 2016

Keywords:
Myricetin
UV–Vis polarization spectroscopy
Linear dichroism
Transition moment directions
Time-dependent density functional theory

ABSTRACT

Myricetin (3,3′,4′,5,5′,7′-hexahydroxyflavone) was investigated by linear dichroism spectroscopy on molecular samples partially aligned in stretched poly(vinyl alcohol) (PVA). At least five electronic transitions in the range 40,000–20,000 cm^{-1} were characterized with respect to their wavenumbers, relative intensities, and transition moment directions. The observed bands were assigned to electronic transitions predicted with TD-B3LYP/6-31 + G(d,p).

1. Introduction

Flavonoids are polyphenolic compounds of herbal origin which are brought into animal organisms by consumption of fruits, vegetables, tea or wine. Apart from their nutritive values, they are distinguished by an impressive spectrum of therapeutic actions [1,2] such as antiinflammatory [3] antimicrobial [4] and anticarcinogenic [5,6], as well as by improving cognitive and motorical functions [7]. Myricetin (MCE), a compound that belongs to the flavonol subclass of flavonoids, displays numerous beneficial impacts on humans [8–11] the most highlighted being its high neuroprotective activity [12] manifested through inhibition of the enzyme that metabolizes the drug used in the treatment of Parkinson's disease and, consequently, increasing its bioavailability and efficiency [13] (Scheme 1).

As for other flavonoids, remarkable antioxidant activity of MCE originates in its capability for free radical scavenging. Even though MCE itself becomes a radical due to this action, the electron delocalization that encompasses planar polycyclic backbone makes the MCE radical one of rather poor reactivity [14]. In addition, six hydroxyl groups enable relatively easy chelation of metal ions which is extremely important when the latter are cell damaging factors.

Successive deprotonation of hydroxyl groups in media of different pH values chemically changes MCE and, consequently, affects its stability and activity [15]. By combining the results obtained from a computational and experimental UV–Vis study, Álvarez-Diduk et al. [16] suggested the most probable mechanism of deprotonation of MCE and demonstrated its decomposition in highly alkaline media (pH ≥ 11). Besides the stability being dictated by the pH value of the surrounding medium, Piantanida et al. found that the stability of MCE in ethanol (EtOH) – water mixture is time-dependent and it decomposes after 2–3 h [17].

The investigations of the activity of MCE generally apply optical spectroscopy as a crucial analytical tool, particularly in the UV–Vis region [15–20]. The electronic transitions of MCE are therefore of considerable interest. Trouillas and coworkers [18] recently performed a theoretical investigation of the UV–Vis spectra for an extensive series of polyphenols, including MCE, focusing on the first strong bands. In order to contribute to the characterization of the electronic transitions of MCE we have investigated the UV–Vis absorption spectrum of the compound in the region 40,000–20,000 cm^{-1} by means of Linear Dichroism (LD) spectroscopy on molecular samples partially aligned in stretched poly(vinyl alcohol) (PVA), thereby providing information on the polarization directions of the electronic transitions [21,22]. The investigation is supported by the application of quantum chemical computational procedures. Additional information is provided as Supplementary material (S1–S10).

2. Calculations

All calculations were performed with the GAUSSIAN09 software package [23]. The equilibrium geometry of MCE was calculated with B3LYP [24,25] density functional theory (DFT) and the 6-31 + G(d,p) basis set [22], using an ultrafine grid (int(grid = ultrafine)) [23] and

☆ This publication is dedicated to Professor Rolf Gleiter on the occasion of his 80th anniversary.

* Corresponding authors.
E-mail addresses: dvojta@irb.hr (D. Vojta), spanget@ruc.dk (J. Spanget-Larsen).

http://dx.doi.org/10.1016/j.saa.2016.09.012
1386-1425/

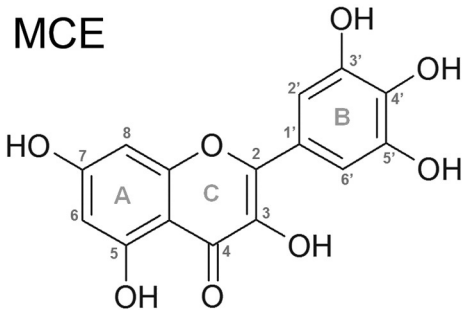

Scheme 1. Structure of myricetin (MCE).

approximating the influence of an alcoholic solvent by the polarized continuum model (PCM) [26] (scrf(pcm,solvent = ethanol)). The most stable conformations of the six hydroxyl groups are found to be those indicated in the molecular diagram in Fig. 1 (detailed structural data and harmonic vibrational wavenumbers are provided as S1). This is consistent with the calculational results of Álvarez-Diduk et al. [16] and with the results of X-ray single crystal and powder diffraction experiments [27]. Starting with a planar geometry (C_s symmetry), a planar molecular structure is predicted with no imaginary frequencies, indicating a true equilibrium structure (S1). However, allowing the molecule to be non-planar leads to the prediction of an equilibrium structure with a slight twist around the 1′–2 bond (linking the pyrogallol and benzopyranone moieties). This is indicated in Fig. 1 which displays the results of a relaxed potential energy scan of the torsional profile, revealing shallow double minima structures close to the torsional angles $\theta = 0°$ and $\theta = 180°$. We have no obvious explanation for the phenomenon; one may speculate that it may be related to different constructions of the integration grid for the (exact) C_s and C_1 symmetries. In the ensuing applications we shall assume that the molecule is effectively planar. Transition to the lowest excited singlet state ($2\ ^1A'$, see below) increases the tendency towards planarity: In the excited state equilibrium geometry, the 1′–2 bond is shortened from 1.466 to 1.426 Å, and the corresponding torsional wavenumber is increased from 4.2 to 12.7 cm^{-1}, relative to the ground state. Geometry optimization of the excited state did not lead to tautomerization, corresponding to Excited State Intramolecular Proton Transfer (ESIPT) [20]. We have not pursued this question further as an ESIPT phenomenon would not be observed in the present absorption spectroscopic experiment.

Vertical transitions to excited singlet electronic states of MCE were computed by using the time dependent TD-B3LYP procedure [28] with the 6-31 + G(d,p) basis set. The influence of the solvent on the calculated transitions was investigated. Following the strategy outlined in ref. [30], a discreet/continuum model was applied, considering a variety of hydrogen bonded MCE-ethanol clusters and representing the influence of the bulk of the solvent by the PCM model (solvent = ethanol). But the influence of explicit solvent molecules on the calculated transitions was found to be of minor importance. In the following we present results obtained with the PCM continuum model, without explicit solvent molecules. This level of approximation provided excellent results for the electronic transitions of hydroxy-anthraquinone dyes [29–31]. A total of 50 excited states were calculated (S3), but we present only detailed results for transitions in the low-energy region of relevance to this study, see Table 1. In-plane transition moment angles φ are given relative to the first strong transition ($2\ ^1A'$), see Fig. 2. Further details are available as Supplementary Data S2 and S3. A gaussian convolution of the predicted transitions is provided as S4; corresponding results obtained with a selection of TD-DFT procedures are given in S5–S10.

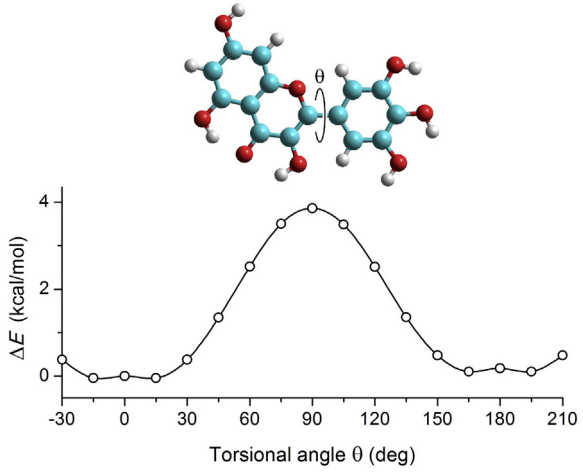

Fig. 1. Torsional potential energy profile for rotation around the 1′–2 bond of myricetin (MCE) computed with B3LYP/6-31 + G(d,p). The torsional angle θ is taken to be zero for the planar conformation indicated.

3. Experimental

3.1. Sample Preparation

A sample of MCE was purchased from Extrasynthese (≥99% purity). Polymer sheet material for LD spectroscopy was prepared from PVA powder with average molecular weight 70,000–100,000 Da (CAS 9002-98-5, Sigma-Aldrich). Five grams of PVA were dissolved in 50 g distilled water at ca. 90 °C while slowly stirring for several hours. After cooling to room temperature, the homogeneous solution was poured onto a glass plate and left to dry for several days. The resulting polymer sheet was cut into samples of 2 × 3.5 cm, and the solute was introduced by immersion of the sample pieces for one week in a concentrated solution of MCE in 96% ethanol (Merck Uvasol). The doped samples were dried, cleaned with methanol (Merck Uvasol) to remove crystals from their surface, and uniaxially stretched ca. 600% in the hot stream of air from a hairdryer. To ensure the reproducibility of the results, a number of replicas were produced and investigated. Reference samples were prepared and treated in exactly the same manner, except for the omission of MCE. Moreover, the stability of MCE in stretched PVA was verified by repeating the measurement after some days; no significant development of the absorption spectrum was observed. Apart from a minor solvent-induced shift, the spectrum observed in PVA compares well with the spectrum observed in EtOH (S4), thereby confirming that MCE is fully protonated in the present experiment [16].

3.2. LD Spectroscopy

UV–Vis LD spectra were recorded at room temperature with a Shimadzu UV-2600 spectrophotometer equipped with rotatable Glan prism polarizers as previously described [30–32]. Two linearly independent absorbance curves were measured, one with the electric vector of the sample beam parallel to the stretching direction (U), and one with the electric vector perpendicular to it (V); in both cases the sample beam was perpendicular to the surface of the PVA sheet. The resulting baseline-corrected absorbance curves are denoted by $E_U(\tilde{\nu})$ and $E_V(\tilde{\nu})$; the difference between them, $E_U(\tilde{\nu}) - E_V(\tilde{\nu})$, is defined as the linear dichroism (LD) [21,22]. An example of the recorded curves is shown in Fig. 3.

4. Results and Discussion

4.1. Linear Dichroism: Orientation Factors and Partial Absorbance Curves

The directional information that can be extracted from the curves $E_U(\tilde{\nu})$ and $E_V(\tilde{\nu})$ (Fig. 3) is provided by the orientation factors K_i